

# Investigating the problem of oscillatory orbits and attractors in wind turbines system under control limits imposed by industry

Sameh A. Eisa

Mechanical and Aerospace Engineering, University of California, Irvine, CA, USA



## ARTICLE INFO

### Keywords:

Wind turbine nonlinear controls  
Oscillations in wind turbines system  
Hopf bifurcation  
Wind turbine  
Mathematical model  
Dynamic behavior  
Small-signal stability

## ABSTRACT

In this paper we investigate whether continuous oscillations are probable for the wind turbines dynamics when connected to the grid. This can have negative consequences on the mechanical parts of the system, the power grid and, possibly, on other power systems connected to the same grid. We consider the wind turbine when the pitch control is activated, exposing it to higher wind speeds. In order to find out if there are continuous oscillations in the state variables that may realistically occur, we investigate if there are periodic attractors for the dynamics that are still allowed within the control limits suggested by many in industry, such as, and not limited to General Electric. The paper provides rigorous mathematical proofs for boundedness of the systems state variables and their derivatives under the imposed control limits by industry. This establishes the existence of attractors in a bounded system under the controls. We then find that there is a Hopf bifurcation in which periodic attractors within the control limits exist. The results are supported by simulations. The nonlinear model used in the analysis is validated versus a real measured data to magnify the finding of this paper. The conclusion of this paper is significant for the nonlinear dynamics and control literature for wind turbines complex system, and the possible consequences on studying/questioning the control limits (limeters) suggested by industry.

## 1. Introduction

According to the US Department of Energy [1], wind is the fastest growing energy resource being used. This rapid expansion requires more scientific research and studies to comprehend the dynamics of Wind Turbine Generators (WTGs), if we are to gain the most from this valuable resource. Governments and corporations are working on understanding the challenges and consequences of integrating WTGs within large cities with/without other power systems. As a result of the complexities of the WTG mechanical and electrical systems, dynamic and control studies have increased recently. This has been observed by the comprehensive review article [2]. Additionally, the reader may consider [3,4] for studies that are looking into the challenges facing the future of power grid with large share of wind and renewable energies.

According to [5], three-bladed (type-3) WTGs are more efficient in extracting power from the air streams, when compared to other types. Coefficients of Performance (curves) of type-3 can go to up 0.4-0.5 efficiency (also see [6]). Most agree that Doubly Fed Asynchronous/Induction Generator (DFAG/DFIG) is mostly the technology used with WTGs systems. A detailed study describing this can be found in the literature review of [2] with citations to many sources in the literature that focus mainly on investigating the implementation and advantageous of DFAG/DFIG technologies. Also, it is noticeable that General Electric (GE)

[7,8] and Electric-Power-Institute/National-Renewable-Energy-Lab (NREL) [9] used DFAG/DFIG-based models in their work. Therefore, we consider Type-3 DFAG/DFIG in our study. In [7] the block diagrams of WTGs were introduced, covering the basic wind power extraction model, rotor models, discussion about the reference speed, pitch control, and reactive power control. In [8], they discuss in greater detail the coefficients of performance ( $C_p$  curves) and added two optional control blocks (active Power and inertia Controls) to make the model more realistic. Summary of GE results can be found in [10]. The GE studies have been validated and compared to measured data in [7,8,11]. Also, the GE team confirmed in their studies the reliability of using their model to represent WTG models for other versions of WTGs. Other modeling, foundation and control literature of WTGs can be found in [12–18].

Having the WTG working under pitch control has been unequivocally the most interesting case to study. This is due the fact that pitch control is only activated when the WTG is exposed to higher wind speeds (see [19–21]). Therefore, a literature of developing, introducing, and improving pitch control, in specific, has emerged in both theoretical and experimental setups. An example of that can be found in [22] for two-bladed WTG, [23] for three-bladed one and [24] for an alternating two-bladed and three-bladed WTG. In [20,25], a WTG model involving pitch control, was introduced and Simulink simulations were done while they cited GE studies mentioned in the previous paragraph, in addition to [26].

E-mail addresses: [seisa@uci.edu](mailto:seisa@uci.edu), [sameheisa235@hotmail.com](mailto:sameheisa235@hotmail.com).

<https://doi.org/10.1016/j.epsr.2019.106098>

Received 30 May 2019; Received in revised form 24 October 2019; Accepted 27 October 2019

Available online 30 November 2019

0378-7796/ © 2019 Elsevier B.V. All rights reserved.

**List of symbols**

$\rho, A_r, v_{\text{wind}}$	air density, rotor area ( $m^2$ ), wind speed (m/s)		
$C_p, w_{\text{ref}}$	aerodynamic power coefficient, reference speed		
$\alpha_{i,j}, P_{\text{mech}}$	empirical constants, mechanical power		
$w_0, w_{\text{base}}$	initial speed, base angular frequency		
$P_{\text{elec}}, V$	electrical (active) power, terminal voltage		
$R, X, E$	infinite bus parameters: resistance, reactance, infinite bus voltage		
$Q_{\text{gen}}, I_{\text{plv}}$	reactive power, active current		
$\lambda, \theta$	tip ratio, pitch angle in degrees		
$w_t, w_g$	dynamic turbine and generator speeds		
$\Delta\theta_m$	integral of difference between dynamic turbine and generator speeds		
$f_1, f_2$	integrals of differences of speeds and powers		
$P_{\text{stl}}, K_{\text{pp}}$	rated power, and pitch control proportional		
$p_{\text{imp}}, P_{\text{elec}}$	power order, filtered electrical power		
$T_{\text{pc}}, K_{\text{ptrq}}$	time constant, torque control proportional		
$V_{\text{ref}}, E_{\text{qcmd}}$	reference voltage, reactive voltage command		
$H, H_g$	turbine inertia constant, generator inertia constant		
$D_{\text{tg}}, K_{\text{vi}}$	shaft damping constant, reactive voltage command time constant		
$K_{\text{itrq}}, K_{\text{pc}}$	torque control gain, pitch compensation proportional		
$K_{\text{ip}}, K_{\text{ic}}$	integral gains		
$K_{\text{pp}}, K_{\text{Qi}}$	pitch control proportional, reference voltage's gain		
$K_{\text{tg}}, T_{\text{pwr}}$	shaft stiffness constant, filtered electric power time		
			constant
		$K_{\text{vi}}, E_q$	reactive voltage command time constant, generator reactive variable
		$\theta_{\text{min}}$	lower control limit of $\theta$
		$\theta_{\text{max}}$	upper control limit of $\theta$
		$\Delta\theta_{\text{mmin}}$	lower bound of $\Delta\theta_m$
		$\Delta\theta_{\text{mmax}}$	upper bound of $\Delta\theta_m$
		$f_{1\text{min}}$	lower bound of $f_1$
		$f_{1\text{max}}$	upper bound of $f_1$
		$f_{2\text{min}}$	lower bound of $f_2$
		$f_{2\text{max}}$	upper bound of $f_2$
		$P_{\text{elecmax}}$	upper bound of $P_{\text{elec}}$
		$P_{\text{elecmin}}$	lower bound of $P_{\text{elec}}$
		$P_{\text{mechmax}}$	upper bound of $P_{\text{mech}}$
		$P_{\text{mechmin}}$	lower bound of $P_{\text{mech}}$
		$V_{\text{max}}$	upper control limit of $V_{\text{ref}}$
		$V_{\text{min}}$	lower control limit of $V_{\text{ref}}$
		$V_{\text{mnm}}$	lower bound of $V$
		$V_{\text{mxm}}$	upper bound of $V$
		$w_{\text{gmax}}$	upper bound of
		$w_{\text{gmin}}$	lower bound of $w_g$
		$X_{\text{LQmax}}$	upper control limit of $E_{\text{qcmd}}$
		$X_{\text{LQmin}}$	lower control limit of $E_{\text{qcmd}}$
		$w_{\text{tmax}}$	upper bound of $w_t$
		$w_{\text{tmin}}$	lower bound of $w_t$

We would like to emphasize that only very recently, large scale nonlinear differential-algebraic models in time domain started to enter the literature to study WTGs dynamics and control. This has been investigated and explained in our very recent series of publications [19,27–32], which for the most part, are time domain transformations of the major models discussed in the previous paragraph (GE [7,8], NREL [9] and [20,25]). In [19], the WTG system was introduced as a differential-algebraic model. In the same paper [19], the WTG full model was reduced to be concerned about the WTG being exposed to higher wind speeds, which is the case when the pitch control is activated and usually is the operating condition in practice. The importance of the study [19] is that the WTG system under pitch control was parametrically studied to identify the parameters that can cause sensitivity problems. The parameters that actually were identified to cause sensitivity, were the wind speed  $v_{\text{wind}}$ , the impedance of the power grid (in particular the reactance  $X$ ). As a result, the paper [27], investigated further the sensitivity study in [19] to see if actually a stability problem may show up consequently. Interestingly, it was found that a drop in  $X$  can cause instability, which introduced the possibility of a bifurcation because of the change in  $X$ . This has been confirmed further in [29], where the eigenvalues were shown sensitive to  $X$  using the same model as in both [19,27]. An interesting observation in both [28,30] is that the algebraic constraint resulting from the network connection to the power grid, can be eliminated through a rigorous mathematical proof as done in [31], and still be accurate in the reduced versions of the model in [28,30]. This accuracy was validated in multiple scale analysis and data validation in [32]. The reader can refer to the detailed explanation of converting the WTGs transfer functions into system of differential-algebraic equations in [21].

### 1.1. The motivation and the objective of this paper

The study in [25] has observed that the system may transition to unstable status when a drop in the impedance occurs. This observation was made in [33], where the possibility of bifurcation and instability was introduced based on eigenvalue sensitivity. The study [27] has investigated this observation further by performing a complete

eigenvalue analysis (local stability analysis) and introduced the existence of a Hopf bifurcation for a severe drop in the reactance  $X$ , while the system had the pitch control activated (WTG exposed to higher wind speeds, which is usually the case of interest). This phenomenon was reported by the NREL in [34] that as the load from the grid reduces, the WTG acts “funny” and “break”. The author of this paper has discussed this observation with the NREL team during his visit to the NREL as a part from the IEEE Green Technology Summit taking place near NREL and with coordination with the lab. In this same conference the papers [27,28] were presented and published. So, can we connect the dots between some of the theoretical investigations ([25,33] and most recently in [27]) in one side, and the practical observation by the NREL [34] in another? This connection of dots can help us understanding how under current control limits (limiters) suggested by industry, the WTG still show this unstable response for large drops in the grid impedance, especially that our recent work [20] raised a lot of questions regarding the limiters themselves and their accuracy. This, consequently, can help us to introduce a new control condition/system that addresses the problem, or at least improve the existing control limiters. The reason why searching for a Hopf bifurcation is useful and desirable for this analysis, is that the Hopf bifurcation can have a family of periodic attractors on one side of the bifurcation point, which causes the oscillations to be consciously happening, bounded and on the attractor or converging to it. This nonlinear dynamical analysis, combined with the control limits effect and NREL observation, has not been investigated (to the best of our knowledge) in the theoretical/practical literature of design, dynamics and control for WTGs. This is kind of expected, as we believe our work [31,32] is the first to provide full rigorous mathematical analysis for the nonlinear dynamics and control of the WTG system. Now, one can see that if the WTG control system and its control limits (limiters) allow for the existence of periodic attractors, and in the same time enforce bounded trajectories, then this can be the explanation for the phenomenon of interest. In another words, the WTG system and its limiters can allow for bounded continuous oscillations when the impedance of the power grid drops, and therefore the WTG shows a strange response even when the limiters are in place. In Section 2 of this paper, we introduce the model for the WTG being exposed to higher



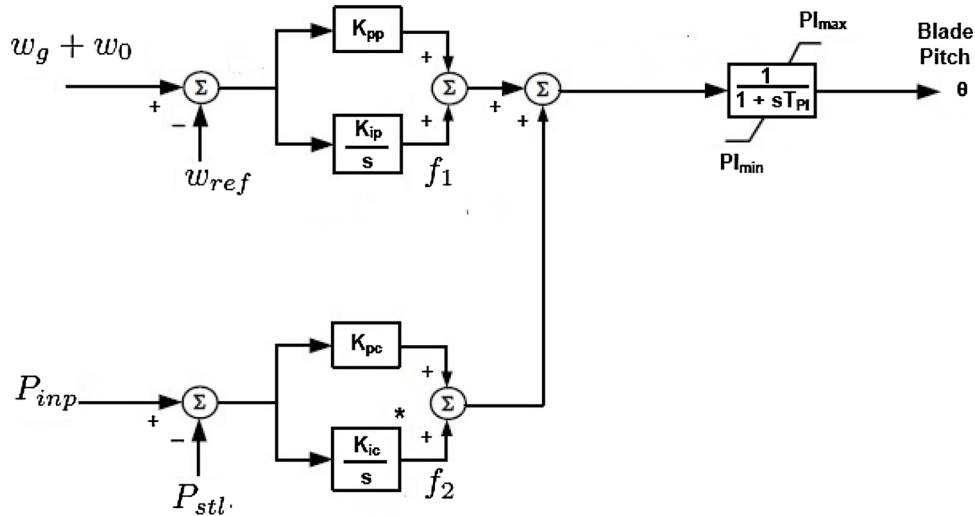


Fig. 2. Pitch control of WTG.

where  $Q_{gen} = V(E_q - V)/X_{eq}$ ,  $Q_{cmd} = \tan(\text{PFE})P_{elec}$ , PFE is small angle,

### 2.3. Comparing our model vs. others and data validation

$$P_{mech} = \frac{1}{2}C_p(\lambda, \theta)\rho A_r v_{wind}^3 = \frac{1}{2}\left(\sum_{i=0}^4 \sum_{j=0}^4 \alpha_{i,j} \theta^i \lambda^j\right)\rho A_r v_{wind}^3,$$

and  $\lambda = (w_t + w_0)/v_{wind}$ . The algebraic constraint can be eliminated by proving that there is a unique solution for Eq. (13) that is representing the dynamics of the system. We introduced the proof in Section 2.2 in [31]. The unique terminal voltage solution is given by

Comparing our model versus others and real measured data would suggest better seriousness of any nonlinear analysis done by this paper. In order to compare the proposed model with another one, we need to select a model that includes most of the WTG control blocks similar to how our model is. The model proposed and studied by [25] mainly cited [26], both of which are highly cited from scholars working on WTGs studies. Therefore, we will focus on one of the differences between the proposed model and the models [25,26]. To test the model used in this paper vs. [25,26] and measured real data, we generated the power-wind profile for all models vs. dynamic measured data for an entire day. Fig. 9 shows this validation and comparison with real measure data. With a large set of dynamic data, it is expected to have the steady state simulations by the models averaging the data fluctuations. It is clear that the model used in this paper averages the data better and fit better the real measured data.

$$V = f(I_{plv}, E_q; X; R; E) = \frac{-B + \sqrt{B^2 - 4AC}}{2A} \quad (14)$$

With  $A = 1 + \frac{2X}{X_{eq}} + \frac{R^2 + X^2}{X_{eq}^2}$ ,  $B = -\left[2I_{plv}R + \frac{2XE_q}{X_{eq}} + \frac{2(R^2 + X^2)E_q}{X_{eq}}\right]$  and  $C = \frac{R^2 + X^2}{X_{eq}} + (R^2 + X^2)I_{plv}^2 - E^2$ .

### 2.2. Verification of the model and comparison with general electric and NREL

### 3. Global boundedness under control limits

We built Simulink models that simulate the blocks and transfer functions similar to the model given by GE [7,8] and NREL [9] to verify the similarity of the results between the Simulink simulations and the numerical solutions of the differential equations (Eqs. (1)–(12) in addition to using Eq. (14)). We built a Simulink model for the system of GE and NREL and ran an autonomous case for a fixed wind speed of  $v_{wind} = 8.2$  m/s. We found the results similar for all the state variables;  $P_{mech}$ ,  $P_{elec}$ , and  $V$ . Fig. 7 shows a sample of the results for  $V$  by setting the initial conditions to be the same in both Simulink and Matlab-ODE15s (numerical solver) and captures the behavior until it settles down to the steady state. The reason we choose this sample is that  $V$  is a direct function of two state variables, the main term to calculate both the active and reactive power, and the most indicative factor for faults. Thus, it is important to capture its behavior. Fig. 8 shows the Simulink project used for simulation. Note that while only one verification figure was given in Fig. 7, all the scopes points in Fig. 8 were tested for similarity with a successful result.

In this section, a rigorous mathematical proof for boundedness of the model's state variables is given in a similar structure to the large scale mathematical proofs given in [31]. However, in this section the proof is only concerned about the model adopted in Section 2. Note that proof of boundedness for a finite dimensional ordinary differential equations system such as the one adopted in this paper, establishes the existence of attractors, as it is widely known in nonlinear dynamical systems theory. Then, it remains to explore numerically if there are periodic attractors that would allow for continuous oscillations under the control limites (limiters) causing the boundedness in the first place. The numerical exploration will be conducted in the next section, while the boundedness proof under control limits is introduced below.

Summary of the control limits imposed by industry, such as in [8], is given in Table 1. The non wind up controls, operator and threshold controls, and physical consequences of the controls (discussed and

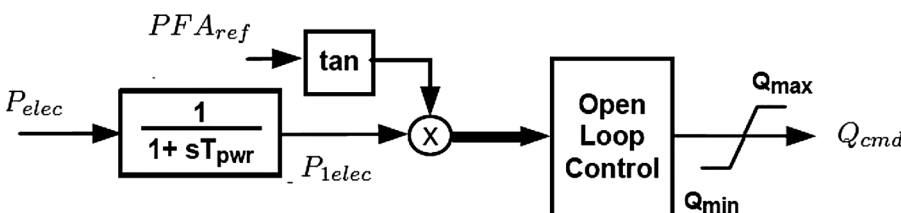


Fig. 3. Reactive power control of WTG.

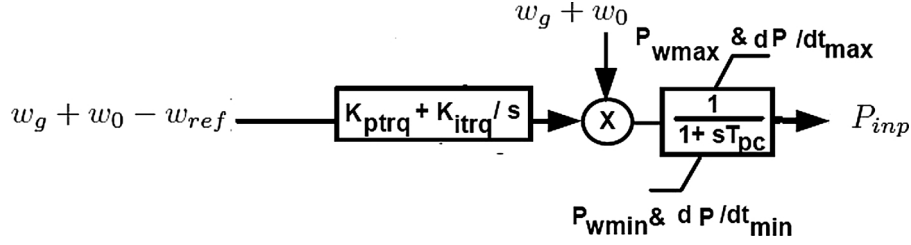


Fig. 4. Powe order of WTG.

explained by details in section 3.1, [31]) give boundedness for the variables  $f_1, f_2, \Delta\theta_m, w_g, w_t, P_{\text{mech}}$ , and  $P_{\text{elec}}$ . Those boundedness leads to the formal listing of condition 1.

**Conditions 1.0.**  $f_1, f_2, \Delta\theta_m, w_g, w_t, P_{\text{mech}}$ , and  $P_{\text{elec}}$  have real lower and upper bounds such that the following inequalities hold:

$$f_{1\min} \leq f_1 \leq f_{1\max}, \quad (15)$$

$$f_{2\min} \leq f_2 \leq f_{2\max}, \quad (16)$$

$$\Delta\theta_{m\min} \leq \Delta\theta_m \leq \Delta\theta_{m\max}, \quad (17)$$

$$w_{g\min} \leq w_g \leq w_{g\max}, \quad (18)$$

$$w_{t\min} \leq w_t \leq w_{t\max}, \quad (19)$$

$$P_{\text{mechmin}} \leq P_{\text{mech}} \leq P_{\text{mechmax}}, \quad (20)$$

$$P_{\text{elecmin}} \leq P_{\text{elec}} \leq P_{\text{elecmax}}. \quad (21)$$

**Remark 1.0.** Boundedness of  $\theta, P_{\text{inp}}, V_{\text{ref}}, E_{q\text{cmd}}, f_1, f_2, \Delta\theta_m$  follow from Table 1 and Conditions 1.0.

**Lemma 1.0.** Suppose  $P_{\text{elec}}, E_q, I_{\text{plv}}$ , and their derivatives are continuous in  $t \in [0, \infty)$ , then we have  $P_{\text{elec}}, E_q$ , and  $I_{\text{plv}}$  are bounded.

**Proof.** From condition (21), we have  $P_{\text{elec}} \in [P_{\text{elecmin}}, P_{\text{elecmax}}]$ , such that Eq. (8) can be rewritten as:

$$\frac{1}{T_{\text{pwr}}} [P_{\text{elecmin}} - P_{\text{elec}}] \leq \frac{dP_{\text{elec}}}{dt} \leq \frac{1}{T_{\text{pwr}}} [P_{\text{elecmax}} - P_{\text{elec}}]$$

Then it follows that:

$$\frac{P_{\text{elecmin}}}{T_{\text{pwr}}} \leq \frac{dP_{\text{elec}}}{dt} + \frac{P_{\text{elec}}}{T_{\text{pwr}}} \leq \frac{P_{\text{elecmax}}}{T_{\text{pwr}}} \quad (22)$$

Multiplying by  $e^{\frac{t}{T_{\text{pwr}}}}$  (the integrator factor), then we get:

$$\frac{P_{\text{elecmin}}}{T_{\text{pwr}}} e^{\frac{t}{T_{\text{pwr}}}} \leq \frac{d[P_{\text{elec}} \cdot e^{\frac{t}{T_{\text{pwr}}}}]}{dt} \leq \frac{P_{\text{elecmax}}}{T_{\text{pwr}}} e^{\frac{t}{T_{\text{pwr}}}} \quad (23)$$

Since  $P_{\text{elec}}, \frac{dP_{\text{elec}}}{dt}$  are continuous in  $t$ , then the function and its derivative are Riemann integrable. By applying  $\int_{t_0}^t () dt$  to the estimate (23), we get:

$$P_{\text{elecmin}} (e^{\frac{t}{T_{\text{pwr}}}} - e^{\frac{t_0}{T_{\text{pwr}}}}) \leq P_{\text{elec}} \cdot e^{\frac{t}{T_{\text{pwr}}}} - P_{\text{elec}}(t_0) \cdot e^{\frac{t_0}{T_{\text{pwr}}}} \leq P_{\text{elecmax}} (e^{\frac{t}{T_{\text{pwr}}}} - e^{\frac{t_0}{T_{\text{pwr}}}}). \quad (24)$$

By rearranging the estimate (24), we get:

$$P_{\text{elecmin}} + e^{\frac{t_0}{T_{\text{pwr}}}} (P_{\text{elec}}(t_0) - P_{\text{elecmin}}) e^{-\frac{t}{T_{\text{pwr}}}} \leq P_{\text{elec}} \leq P_{\text{elecmax}} + e^{\frac{t_0}{T_{\text{pwr}}}} (P_{\text{elec}}(t_0) - P_{\text{elecmax}}) e^{-\frac{t}{T_{\text{pwr}}}}. \quad (25)$$

Then as  $t \rightarrow \infty$ ,  $P_{\text{elec}}$  is bounded such that:

$$P_{\text{elecmin}} \leq P_{\text{elec}} \leq P_{\text{elecmax}}. \quad (26)$$

Boundedness for  $P_{\text{elec}}$  can be shown independent on  $t$  as,

$$|P_{\text{elec}}| \leq |P_{\text{elecmax}}| + \left| e^{\frac{t_0}{T_{\text{pwr}}}} (P_{\text{elec}}(t_0) - P_{\text{elecmax}}) \right| \quad \forall t. \quad (27)$$

From Table 1, Eqs. (11) and (12), and following similar steps as the previous boundedness proof in estimates (22)–(26) we get:

$$|E_q| \leq |X|_{Q\text{max}} + \left| e^{\frac{t_0}{0.02}} (E_q(t_0) - |X|_{Q\text{max}}) \right| \quad \forall t, \quad (28)$$

and,

$$|I_{\text{plv}}| \leq |I_{\text{pmax}}| + \left| e^{\frac{t_0}{0.02}} (I_{\text{plv}}(t_0) - I_{\text{pmax}}) \right| \quad \forall t. \quad (29)$$

This proves Lemma 1.0.

**Results 1.0.** Boundedness of  $f_1, w_g, w_t, \Delta\theta_m, P_{\text{inp}}, P_{\text{elec}}, V_{\text{ref}}, E_{q\text{cmd}}, E_q, I_{\text{plv}}, f_2$ , and  $\theta$  implies the boundedness of their derivatives. This follows directly by applying the absolute value for the derivatives in Eqs. (1)–(12) with  $V$  as in Eq. (14).

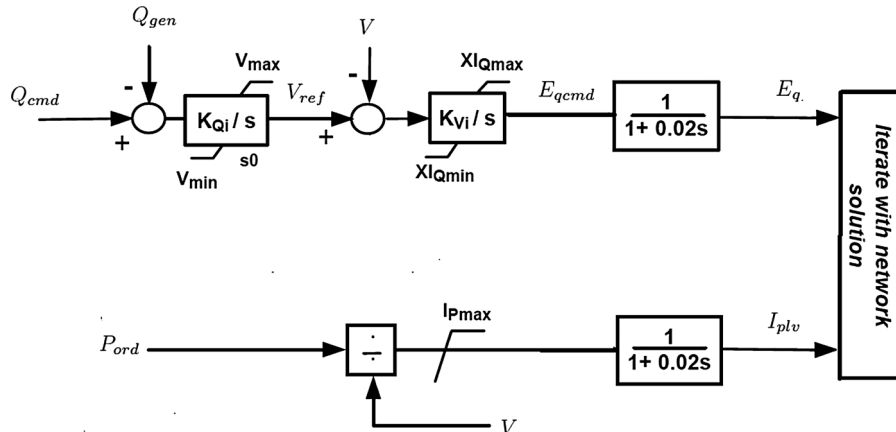


Fig. 5. Electrical control of WTG.

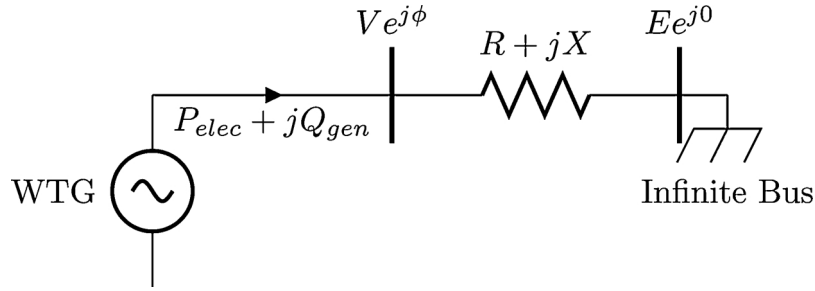


Fig. 6. Single-Machine Infinite-Bus test system.

**Theorem 1.0.** The system given in Eqs. (1)–(12) with  $V$  as in Eq. (14), has globally bounded state variables and derivatives.

**Remark 1.1.** The proof for Theorem 1.0 follows from Table 1, Lemma 1.0, and Remark 1.0.

## 4. Hopf bifurcation and periodic attractors

### 4.1. Hopf bifurcation

Since we proved boundedness for the state variables and derivatives of the system, we have a working dynamics under the control limits in which things change in a bounded way, which protects the electrical and mechanical components from many problems. Based on eigenvalues calculations in [19], the system guarantees local stability for the full range of wind speeds and their steady states. However, the same paper suggested that eigenvalues and state variables are sensitive to some of the system's parameter, in particular,  $v_{wind}$  and the grid parameters such as  $X$  and  $R$ . The eigenvalues were sensitive to  $v_{wind}$ , but the local stability not shown to be affected. Since the wind turbine is assumed to be connected to the grid, then a drop in  $R$  or  $X$  values is realistically possible. In order for us to understand that possibility, we focused on a high resolution rectangle in  $R$  and  $X$  space. We built a code that discretized the domain in  $R$  and  $X$  space. For every given point, the code linearizes and computes the eigenvalues. The results suggest that there are unstable steady states for very small values. Based on our trial, we found that for  $R \in [0.01-0.03]$  (include the sample value of  $R$  given in [19–21,27]), steady states transitioned from unstable at  $X = 0.0021$  to stable at  $X = 0.0022$ . We noticed a drop from the sample value of  $X = 0.02987$  to  $\frac{X}{15} = 0.00199$  with the same sample value of  $R$  taking the steady state from a stable state to an unstable one. The code then focused in to test values of  $X$  in order of  $10^{-16}$  accuracy to get as close as possible to the transitioning point as Matlab's sensitivity allows.

We found that the transitioning point is between  $X_1 = 0.00213181671283$  (Unstable) and  $X_2 = 0.0021318167128341$  (Stable). Table 2 shows the eigenvalues' computation at those two values of  $X$ .

Assuming that  $\text{Real}(\lambda_{9,10}) \in C(X)$ ,  $\forall X \in [X_1, X_2]$  (as in Table 2) then by the Intermediate Value Theorem  $\exists X^* \in [X_1, X_2]$  s. t.  $\exists \text{Real}(\lambda_{9,10}) = 0$ . This is one of the indications that there is a Hopf bifurcation. Since the system is 12 by 12 nonlinear differential equations, it might be hard to do further analytical verification for the existence of Hopf bifurcation. Therefore, we solve this numerically and try to observe the behavior of solutions near the transition point of  $X$  while fixing  $R$ . If this is a Hopf bifurcation, a family of periodic attractors, leading to continuous oscillations, are expected to exist in the neighborhood of the bifurcation point. Our numerical simulations identified that, it is the case, we do have a Hopf bifurcation.

### 4.2. Periodic attractors under control limits

Since we have a Hopf bifurcation, the important part now is whether the family of periodic attractors would cause the system to have oscillations under the control limits given in Table 1. What we have found is that there exists a family of periodic attractors corresponding to neighboring values of  $X$  on the unstable side of the bifurcation in which the attractor is under the allowed control limits!

To strengthen our point, we ran a numerical solution for the system with an initial condition of  $1.001\vec{x}_{state}$ , where  $\vec{x}_{state}$  is the vector of the system's steady state when  $X = X_1$ . We ran the code for 30,000 time units. Figs. 10–12 illustrate the results for  $V_{ref}$ ,  $E_{qcmd}$ , and  $I_{plv}$ . Note that the simulations close to a the Hopf point can be very tricky. One has to be careful and keeping in mind that simulations with small time units may mislead the observer as trajectories can be extremely slow. For instance, let us run the simulation represented in Fig. 10, with zoomed in time units, one trial with a 10,000 time units (Fig. 13) and another trial with 100 time units (Fig. 14), instead of 30,000 time units. It is clear that the information we get from the zoomed in simulations are

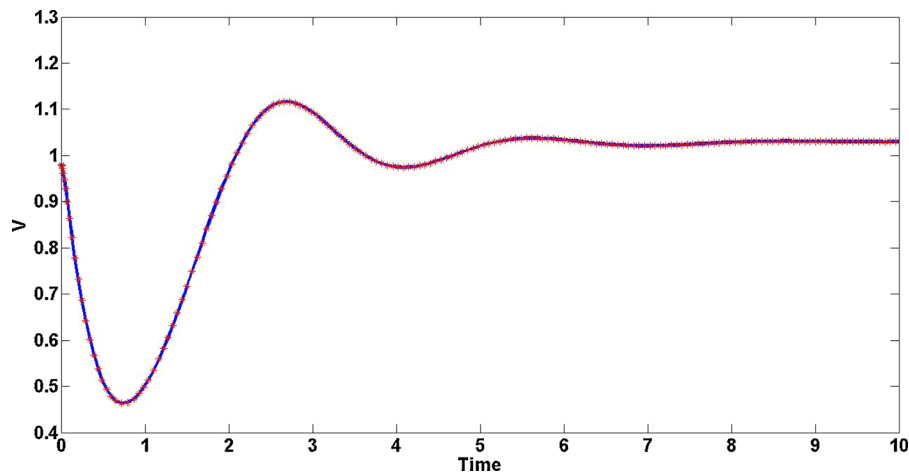


Fig. 7. Response of implementations in Matlab ODE15s solver (solid line) and Simulink simulation (stars) to the same initial conditions.

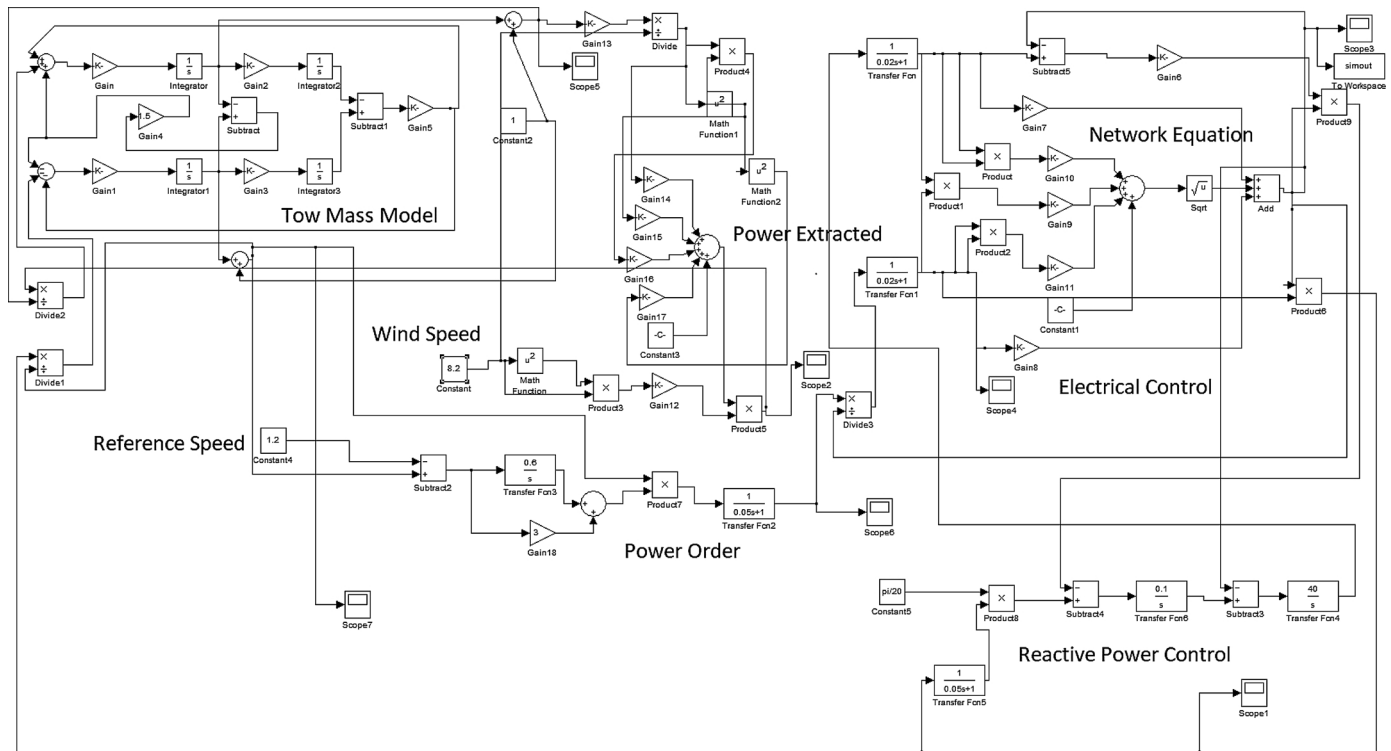


Fig. 8. Simulink project for a fixed wind speed trial.

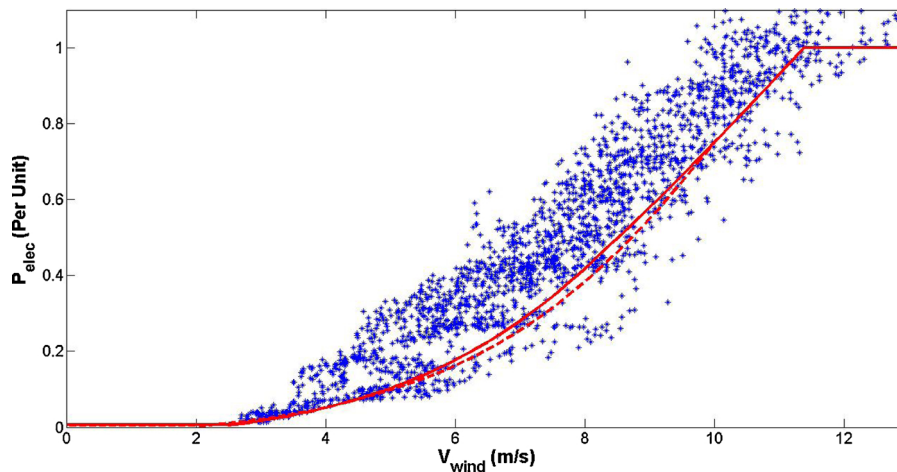


Fig. 9. Real data of a WTG (stars) vs. power-wind speed curves for the proposed model (solid) and [25,26] (dashed).

Table 1  
Control limits to be applied.

Variable	Lower bound	Upper bound
$Q_{cmd}$	$Q_{min} = -0.436$	$Q_{max} = 0.436$
$V_{ref}$	$V_{min} = 0.9$	$V_{max} = 1.1$
$E_{qcmd}$	$XI_{Qmin} = 0.5$	$XI_{Qmax} = 1.45$
$\frac{I_{plv}}{V}$	$I_{pmin} > 0$	$I_{pmax} = 1.1$
$\theta$	$\theta_{min} = 0$	$\theta_{max} = 27$
$P_{inp}$	$P_{wmin} = 0.04$	$P_{wmax} = 1.12$
$\frac{dP_{inp}}{dt}$	$dP_{min} = -0.45$	$dP_{max} = 0.45$
$\frac{d\theta}{dt}$	$d\theta = -10$	$d\theta = 10$

Table 2  
Eigenvalues for two different values of  $X$  around a suspected bifurcation with  $R = 0.02$ .

$X_1 = 0.00213181671283$	$X_2 = 0.0021318167128341$
$\lambda_1 = -52.6079$	$\lambda_1 = -52.6079$
$\lambda_2 = -50.0344$	$\lambda_2 = -50.0334$
$\lambda_3 = -20$	$\lambda_3 = -20$
$\lambda_4 = -16.1189$	$\lambda_4 = -16.1189$
$\lambda_{5,6} = -1.3504 \pm 12.1006i$	$\lambda_{5,6} = -1.3504 \pm 12.1006i$
$\lambda_{7,8} = -0.3692 \pm 0.7489i$	$\lambda_{7,8} = -0.3692 \pm 0.7489i$
$\lambda_{9,10} = 97 \times 10^{-14} \pm 2.2733i$	$\lambda_{9,10} = -5 \times 10^{-15} \pm 2.2733i$
$\lambda_{11} = -2.7717$	$\lambda_{11} = -2.7717$
$\lambda_{12} = -0.1503$	$\lambda_{12} = -0.1503$

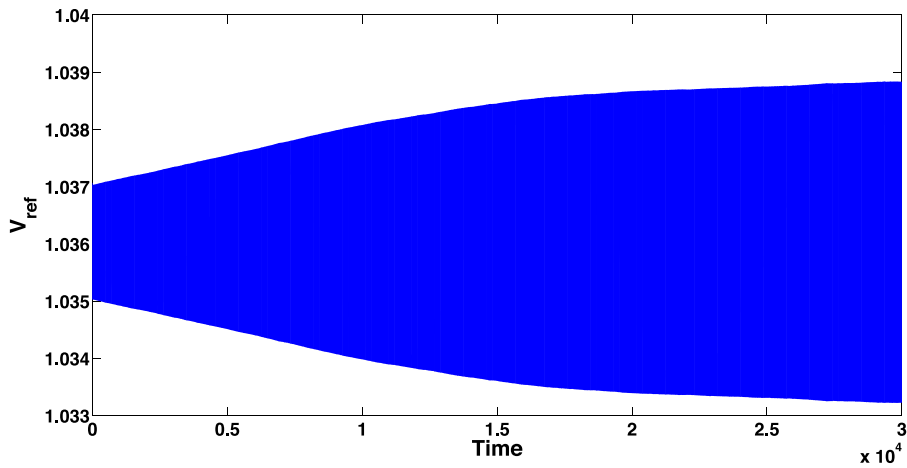


Fig. 10.  $V_{ref}$  approaching a periodic attractor without exceeding the control limits.

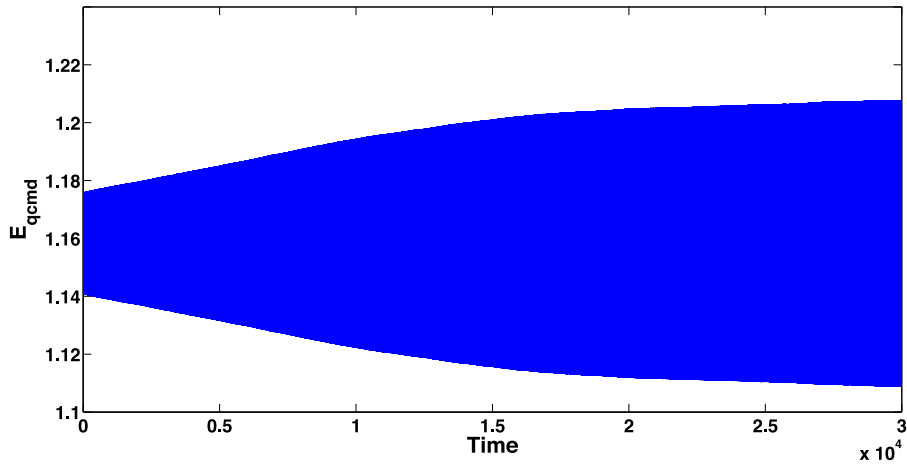


Fig. 11.  $E_{qcmd}$  approaching a periodic attractor without exceeding the control limits.

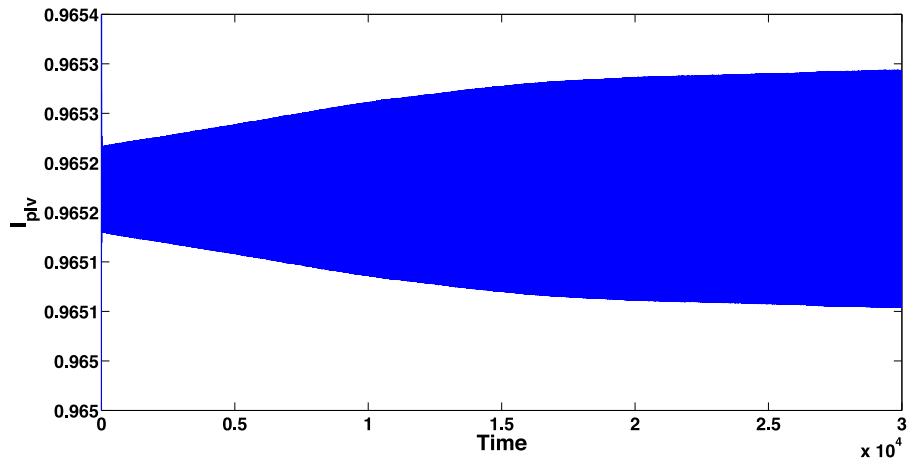


Fig. 12.  $I_{plv}$  approaching a periodic attractor without exceeding the control limits.

misleading as they may indicate a completely inaccurate conclusions, such as reaching a settled oscillation (attractor) that is not the right one, which is the case of Fig. 14, or wrongfully trick us to think we have instability (divergent oscillations) in the case of Fig. 13. Therefore, we have made the choice for 30,000 time units in our simulations after even trying excessively larger time units with the same results.

#### 4.3. Periodic attractors out of control limits

It is expected that, as we get further away from the bifurcation point

on the unstable side, the periodic orbits will be wider. At some point they will exceed the control limits, which means that the limiters will be enforced before the solutions make it to the attractors. We repeated the same trial we had in the last subsection, but with 10,000 time units at  $X = 0.0021$ . Figs. 15–18 illustrate the result for  $\theta$ ,  $V_{ref}$ ,  $E_{qcmd}$ , and  $I_{plv}$ .

#### 4.4. Discussion and observations

Let's start the discussion by Figs. 19 and 20, as where we can see both  $E_{qcmd}$  and  $V_{ref}$  plotted together. The resulting graphs represent

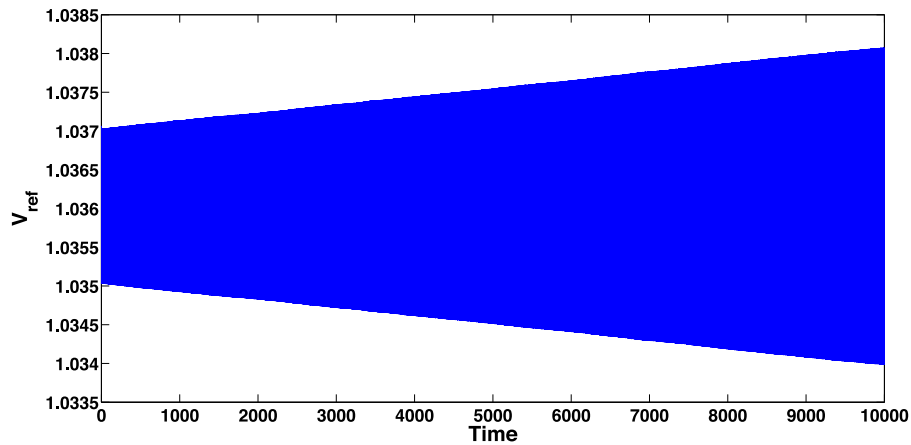


Fig. 13.  $V_{ref}$  appears wrongly to be in a divergent oscillation.

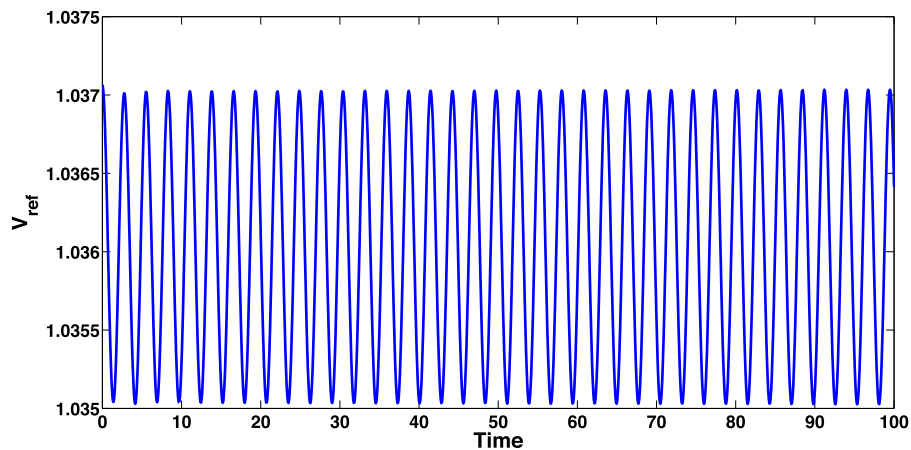


Fig. 14.  $V_{ref}$  approaching appears wrongly to have reached a periodic attractor.

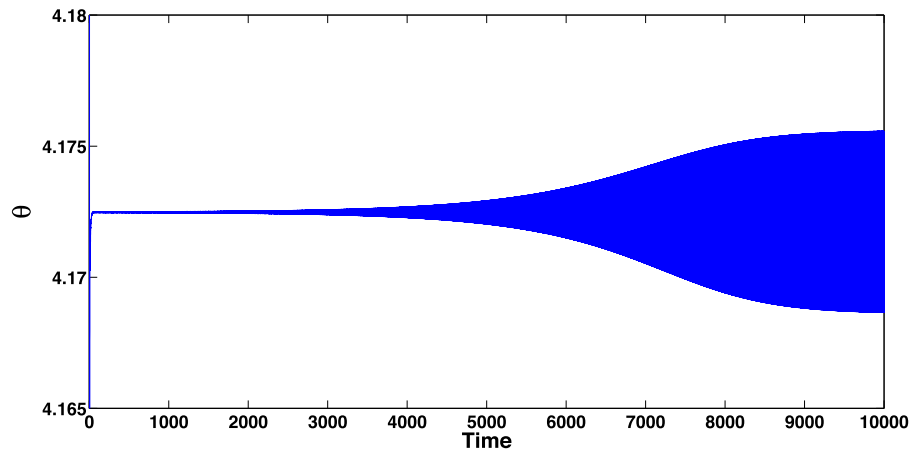


Fig. 15.  $\theta$  approaching a periodic attractor exceeding the control limits.

periodic orbits that are the result of running the simulation for 30,000 time units with  $1.001\vec{x}_{state}$ . As we observed in the past two trials in the past two subsections, one of the periodic attractors is fully under the control limits while the other one is fully out. We expect then that there is a family of periodic attractors that are allowed under the control limits. Given that the initial condition is a negligible disturbance of the steady state (the order of  $10^{-3}$ ), we see that the wind turbine state variables can enter a state of continuous oscillations that will have a great effect on  $E_{qcmd}$  and, therefore, the generator variable  $E_q$  (see Eq. (11)). Another generator and grid variable that is affected is  $I_{plv}$ . Also,

the oscillations are relatively high for  $V_{ref}$ , which directly affects the terminal voltage  $V$  (see Eq. (9)). This will make the wind turbine connection with the grid unstable from an engineering point of view and have unwanted effects on the other power systems interacting with the wind turbine in the common grid.

We observed that the most oscillating variables are  $E_{qcmd}$  and  $V_{ref}$ . We noticed that those variables have the highest weights in the eigenvectors corresponding to the eigenvalues  $\lambda_{9,10}$  (see Table (2)). As noticed from Eqs. (9) and (11), the oscillation effect will occur in  $E_q$  and  $V$ . We observed small oscillations with  $\theta$ , which can cause mechanical

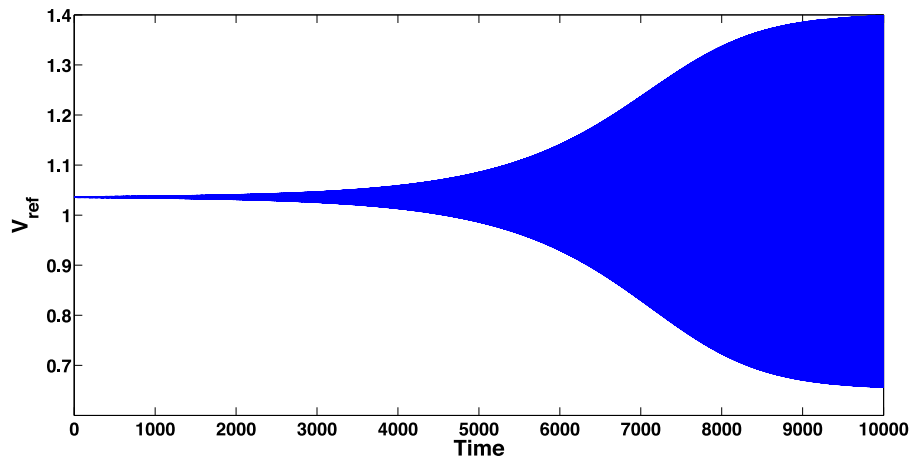


Fig. 16.  $V_{ref}$  approaching a periodic attractor exceeding the control limits.

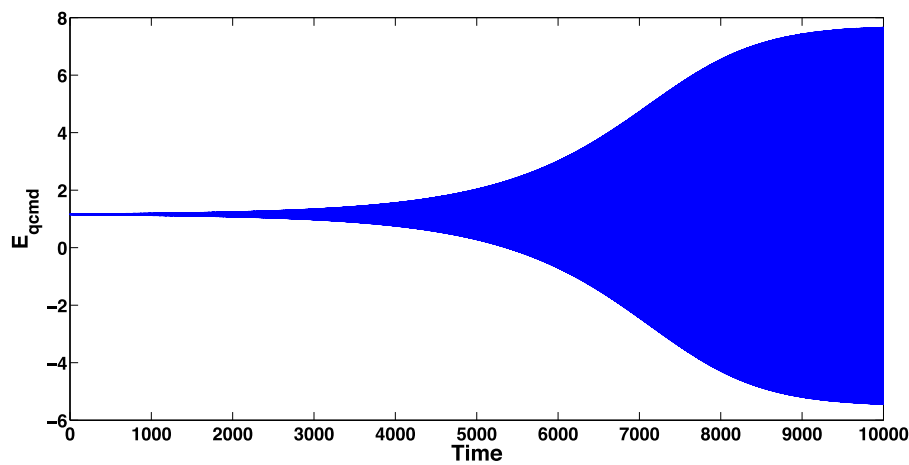


Fig. 17.  $E_{qcmd}$  approaching a periodic attractor exceeding the control limits.

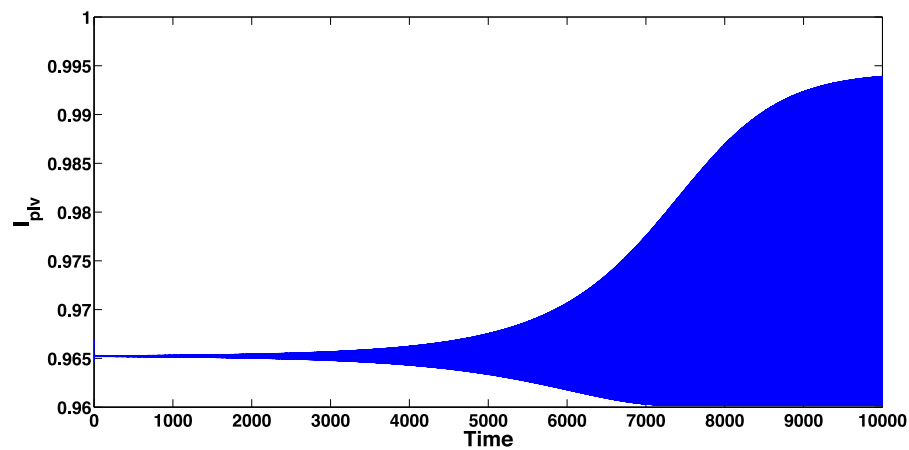


Fig. 18.  $I_{plv}$  approaching a periodic attractor exceeding the control limits.

problems to the pitch mechanism.  $I_{plv}$  has a small oscillation as well. The oscillations are stronger as we get further from the bifurcation point, so they are stronger with  $X = 0.0021$  for example.

#### 4.5. Connecting the dots

One can see now that after establishing the existence of attractors analytically in Section 3, numerically it is tested and found that there are periodic attractors taking place under the allowable control limits

for small values of  $X$ . This should be an explanation to what was discussed in the introduction about the motivating problem for this paper. The current imposed control limits and control design of the WTG allows for strange response in the case the impedance of the power grid drops. Now the finding of this paper suggests that this phenomenon, which is reported by the NREL [34], can be theoretically tracked, especially that the model used in this paper is verified and validated versus GE, NREL and real data. Research should reveal more how to move the bifurcation curve, so that the family of periodic attractors can

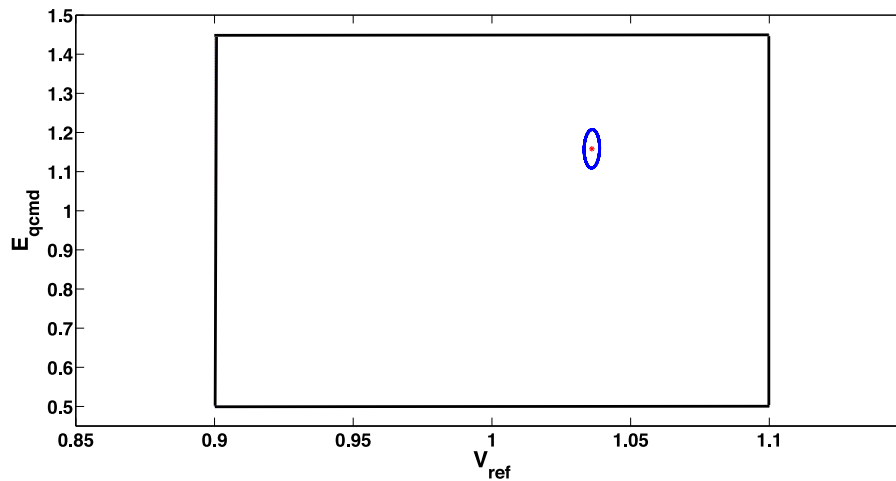


Fig. 19.  $E_{qcmd}$  plotted vs.  $V_{ref}$  at  $X = 0.00213181671283$  approaching a periodic attractor (blue), control limits (black), and initial condition (red star).

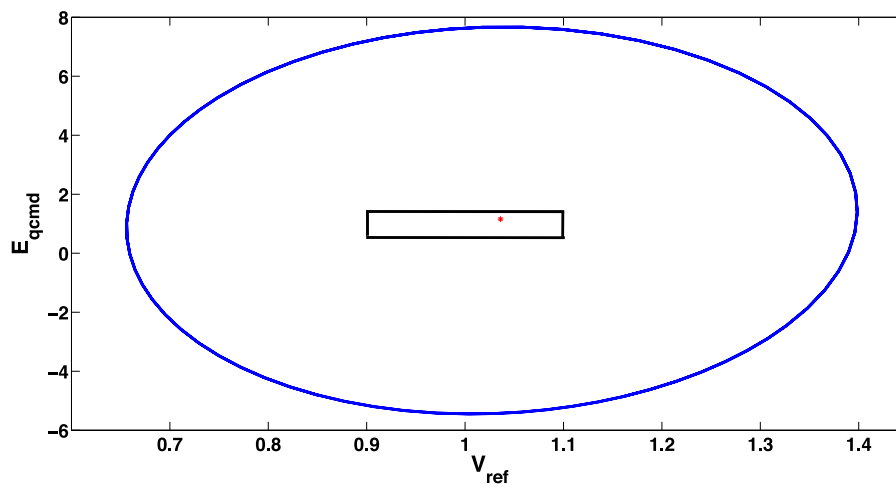


Fig. 20.  $E_{qcmd}$  plotted vs.  $V_{ref}$  at  $X = 0.0021$  approaching a periodic attractor (blue), control limits (black), and initial condition (red star).

be fully, or at least optimally, eliminated. Also, it may be important to study the effect of changing the control limits (mentioned in [20]) and/or adding more controls between the WTG and the power grid to eliminate this issue.

## 5. Conclusion

Wind turbines dynamics and control with the pitch activated under control limits is mathematically analyzed. This analysis was through proof of boundedness of the system's state variables and their derivatives under the control limits proposed by GE. Under the control limits, the dynamics have a Hopf bifurcation, which allows the existence of periodic attractors. We have shown a case for  $X$  value in which continuous oscillations happen and cannot be stopped by the control limits imposed by industry, because it is bounded within them. This explains what the NREL reported about the WTG that it responds strangely to low power grid impedance. We also presented a case in which the periodic attractors can be prevented by the control limits as they exceed them. These results, which are crucial in understanding the nonlinear behavior of current WTGs, need to be seriously addressed among the community members and further studied if we are to implement wind turbines into the common power grid with other power systems, and in large scale. Noting that the model used in this paper is compared and validated versus manufacturers models and real data, the seriousness of the claims made by this paper are more likely to be captured practically. Also, more effort needs to be done to communicate findings like

these in this paper with industry for further experimentation and validations.

## Conflict of interest

The author of this paper has no conflict of interest to declare.

## Acknowledgment

The author of this paper would like to thank The North American Wind Research and Training Center for sharing data with New Mexico Tech through Dr. Kevin Wedeward, which have been used originally in [20,21,32] and regenerated Fig. 9. For more information about the data used, please see: <http://www.mesalands.edu/news-releases/the-north-american-wind-research-and-training-center-shares-data-with-new-mexico-tech-to-enhance-the-future-research-of-wind-energy-technology/>.

## References

- [1] Department of Energy, Energy Dept. Reports: U.S. Wind Energy Production and Manufacturing Reaches Record Highs, (2013) (accessed 25.09.15), <http://energy.gov/articles/energy-dept-reports-us-wind-energy-production-and-manufacturing-reaches-record-highs>.
- [2] M. Rahimi, Dynamic performance assessment of dfig-based wind turbines: a review, *Renew. Sustain. Energy Rev.* 37 (2014) 852–866.
- [3] H. Lund, Large-scale integration of wind power into different energy systems,

- Energy 30 (13) (2005) 2402–2412.
- [4] H. Lund, B.V. Mathiesen, Energy system analysis of 100% renewable energy systems – the case of Denmark in years 2030 and 2050, *Energy* 34 (5) (2009) 524–531.
- [5] S. Heier, *Grid Integration of Wind Energy Conversion Systems*, 2nd ed., John Wiley & Sons, 2006.
- [6] A. Tummala, R.K. Velamati, D.K. Sinha, V. Indrāja, V.H. Krishna, A review on small scale wind turbines, *Renew. Sustain. Energy Rev.* 56 (2016) 1351–1371.
- [7] N.W. Miller, W.W. Price, J.J. Sanchez-Gasca, *Dynamic Modeling of GE 1.5 and 3.6 Wind Turbine-Generators*, General Electric International, Inc., 2003 October Report.
- [8] K. Clark, N.W. Miller, J.J. Sanchez-Gasca, *Modeling of GE Wind Turbine-Generators for Grid Studies*, General Electric International, Inc., 2010 April, Report.
- [9] P. Pourbeik, *Specification of the Second Generation Generic Models for Wind Turbine Generators*, Electric Power Research Institute, 2014 January, Report.
- [10] N. Miller, J. Sanchez-Gasca, W. Price, R. Delmerico, *Dynamic modeling of GE 1.5 and 3.6 MW wind turbine-generators for stability simulations*, 2003 IEEE Power Engineering Society General Meeting (2003).
- [11] J.M. MacDowell, K. Clark, N.W. Miller, J.J. Sanchez-Gasca, *Validation of GE wind plant models for system planning simulations*, 2011 IEEE Power and Energy Society General Meeting (2011).
- [12] J.G. Slootweg, H. Polinder, W.L. Kling, *General model for representing variable speed wind turbines in power system dynamics simulations*, *IEEE Trans. Power Syst.* 18 (1) (2003) 144–151.
- [13] S.A. Eisa, *Mathematical Modeling and Analysis of Wind Turbines Dynamics*, New Mexico Institute of Mining and Technology, 2017 Ph.D. Thesis.
- [14] I.A. Hiskens, *Dynamics of type-3 wind turbine generator models*, *IEEE Trans. Power Syst.* 27 (1) (2012) 465–474.
- [15] A.M. Boulamatsis, T.K. Barlas, H. Stapountzis, *Active control of wind turbines through varying blade tip sweep*, *Renew. Energy* 131 (2019) 25–36.
- [16] X. Wu, Y. Hu, Y. Li, J. Yang, L. Duan, T. Wang, T. Adcock, Z. Jiang, Z. Gao, Z. Lin, et al., *Foundations of offshore wind turbines: a review*, *Renew. Sustain. Energy Rev.* 104 (2019) 379–393.
- [17] S. Haigh, *Foundations for offshore wind turbines, ICPMG2014 – Physical Modelling in Geotechnics: Proceedings of the 8th International Conference on Physical Modelling in Geotechnics 2014 (ICPMG2014)*, Perth, Australia, 14–17 January 2014, CRC Press, 2019, p. 153.
- [18] J.M.M. Guerrero, C. Lumberras, D. Reigosa, D. Fernandez, F. Briz, C. Blanco, *Accurate rotor speed estimation for low-power wind turbines*, *IEEE Trans. Power Electron.* (2019).
- [19] S.A. Eisa, K. Wedeward, W. Stone, *Sensitivity analysis of a type-3 dfig wind turbine's dynamics with pitch control*, 2016 IEEE Green Energy and Systems Conference (IGSEC) (2016) 1–6, <https://doi.org/10.1109/IGESC.2016.7790064>.
- [20] S.A. Eisa, *Modeling dynamics and control of type-3 dfig wind turbines: Stability, q droop function, control limits and extreme scenarios simulation*, *Electr. Power Syst. Res.* 166 (2019) 29–42.
- [21] S.A. Eisa, *Nonlinear modeling, analysis and simulation of wind turbine control system with and without pitch control as in industry*, *Advanced Control and Optimization Paradigms for Wind Energy Systems*, Springer, 2019, pp. 1–40.
- [22] E. van Solingen, J.-W. van Wingerden, *Linear individual pitch control design for two-bladed wind turbines*, *Wind Energy* 18 (4) (2015) 677–697.
- [23] M.G. Molina, P.E. Mercado, *Modelling and control design of pitch-controlled variable speed wind turbines*, *Wind Turbines*, In Tech, 2011.
- [24] I. Hayat, T. Chatterjee, H. Liu, Y.T. Peet, L.P. Chamorro, *Exploring wind farms with alternating two-and three-bladed wind turbines*, *Renew. Energy* 138 (2019) 764–774.
- [25] G. Tsourakis, B. Nomikos, C. Vournas, *Effect of wind parks with doubly fed asynchronous generators on small-signal stability*, *Electr. Power Syst. Research* 79 (1) (2009) 190–200.
- [26] W.G. C4.601, *Modeling and Dynamic Behavior of Wind Generation as It Relates to Power System Control and Dynamic Performance*, (2007) August, Report, CIGRE TB 328.
- [27] S.A. Eisa, W. Stone, K. Wedeward, *Mathematical modeling, stability, bifurcation analysis, and simulations of a type-3 dfig wind turbine's dynamics with pitch control*, 2017 Ninth Annual IEEE Green Technologies Conference (GreenTech) (2017) 334–341, <https://doi.org/10.1109/GreenTech.2017.55>.
- [28] S.A. Eisa, K. Wedeward, W. Stone, *Time domain study of a type-3 dfig wind turbine's dynamics: Q drop function effect and attraction vs control limits analysis*, 2017 Ninth Annual IEEE Green Technologies Conference (GreenTech) (2017) 350–357, <https://doi.org/10.1109/GreenTech.2017.57>.
- [29] S.A. Eisa, *Local study of wind turbines dynamics with pitch activated: trajectories sensitivity*, 2017 IEEE Green Energy and Smart Systems Conference (IGESSC) (2017) 1–6, <https://doi.org/10.1109/IGESC.2017.8283448>.
- [30] S.A. Eisa, W. Stone, K. Wedeward, *Dynamical study of a type-3 dfig wind turbine while transitioning from rated speed to rated power*, 2017 IEEE Green Energy and Smart Systems Conference (IGESSC) (2017) 1–6, <https://doi.org/10.1109/IGESC.2017.8283452>.
- [31] S.A. Eisa, W. Stone, K. Wedeward, *Mathematical analysis of wind turbines dynamics under control limits: boundedness, existence, uniqueness, and multi time scale simulations*, *Int. J. Dyn. Control* 6 (3) (2018) 929–949.
- [32] S.A. Eisa, K. Wedeward, W. Stone, *Wind turbines control system: nonlinear modeling, simulation, two and three time scale approximations, and data validation*, *Int. J. Dyn. Control* 6 (4) (2018) 1776–1798.
- [33] L. Yang, Z. Xu, J. Ostergaard, Z.Y. Dong, K.P. Wong, X. Ma, *Oscillatory stability and eigenvalue sensitivity analysis of a dfig wind turbine system*, *IEEE Trans. Energy Convers.* 26 (1) (2011).
- [34] A. Bowen, A. Huskey, H. Link, K. Sinclair, T. Forsyth, D. Jager, *Small wind turbine testing results from the national renewable energy lab*, The American Wind Energy Association WINDPOWER 2009 Conference and Exhibition, Chicago, IL, 2009.